Academic Journal of Science and Technology
ISSN: 2771-3032 | Vol. 19, No. 1, 2026

Biodynamic Modelling of the Glove-arm System

Yumin Ji *

School of Mechanical Engineering, University of Shanghai for Science and Technology, Shanghai, China
*** Corresponding author Email:** 1289737468@qq.com

Abstract: Occupational exposure to the hand-transmitted vibration causes health problems and difficulties in the operators of hand-held power tools. Arm vibration can be effectively controlled by wearing vibration-damping gloves. In this study, a biodynamic glove-arm system model is developed to predict the vibration transmission rate when using such gloves. The arm system is segmented into substructures—including the index finger, middle finger, palm, forearm, upper arm, and shoulder—which are interconnected by linear stiffness and damping elements. The glove is represented by seven mass blocks, each attached to the index finger, middle finger, palm, finger skin, palm skin, and both sides of the tool handle. The root-mean-square error between the experimentally measured and model-predicted transfer rates is used as the objective function for parameter identification, employing a particle swarm optimization (PSO) multi-objective error minimization approach. Simulation results demonstrate that the fitted vibration transfer rates for each segment closely match the experimental data, validating the effectiveness of the proposed model.

Keywords: Biomechanical Modeling; Hand-Arm-System; Pso; Vibration Damping Gloves.

1. Introduction

Long-term vibration generated by hand-held power tools is associated with multiple adverse effects on the vascular, musculoskeletal, and nervous systems, commonly described as Hand–Arm Vibration Syndrome (HAVS) [1]. The symptoms of HAVS include pain, numbness, lack of hand strength and reduced dexterity. HAVS has a profound impact on the functional, social, emotional and psychological aspects of the patient's life, not only in terms of physical disability, but also in terms of identity and quality of life [2] .

A wide range of biomechanical models has been developed to investigate the vibration behavior of the hand–arm system during interaction with power tools. Rakheja [3] constructed twelve different biomechanical representations to systematically analyze tool-induced vibrations, emphasizing the need for accurate vibration characterization and reliable evaluation frameworks for vibration attenuation. Dong [4] introduced a five-degree-of-freedom biodynamic model and, through a combination of experimental measurements and analytical modeling, demonstrated that vibration transmission is strongly frequency-dependent, with high-frequency components mainly affecting the fingers and hand, while lower-frequency vibrations propagate toward the arm and shoulder. Adewusi [6] further extended posture-dependent modeling by proposing six- and seven-degree-of-freedom biodynamic models for bent- and extended-arm configurations, respectively, enabling simultaneous assessment of impedance and vibration transmissibility. In addition, Dong [7] developed a coupled grinder–workpiece–hand–arm model, revealing that workpiece resonance is primarily governed by the workpiece mass and contact stiffness, and showing that anti-vibration gloves, although capable of reducing vibration transmission to the hand–arm system, may also increase workpiece resonance under certain conditions. More recently, Wang [8] proposed a hybrid biomechanical modeling approach combining multibody dynamics and finite element methods to simultaneously predict grip force, interface pressure distribution, and vibration transmission characteristics, with applications mainly focused on forklift steering wheel systems.

Table 1. Substructure

	Substructure		
m_{f1}	Index Finger Bone Mass	K_e	Elbow-lumped rotational stiffness of the upper arm
m_{f2}	Middle Finger Bone Mass	K_s	Rotational stiffness of shoulder joint
m_p	Bone mass associated with the palm and adjacent regions	K_b	Pelvic-joint-lumped rotational stiffness of the trunk
m_{tp}	Soft tissue mass of the skin over the fingers	c_1	Finger damping coefficient
m_{tf}	Soft tissue mass of the skin over the palm	c_2	Finger damping coefficient
m_{fa}	Total biological mass of the forearm segment	c_3	Index finger–palm damping coefficient
m_{ua}	Total biological mass of the upper arm segment	c_4	Middle finger–palm damping coefficient
k_1	Index finger linear stiffness	c_w	Wrist damping coefficient
k_2	Middle finger linear stiffness	c_e	Elbow damping coefficient
k_3	Index finger–palm linear stiffness	c_s	Shoulder damping coefficient
k_4	Middle finger–palm linear stiffness	C_e	Elbow-lumped damping of the upper arm
k_w	Wrist linear stiffness	C_s	Shoulder joint damping coefficient
k_e	Elbow linear stiffness	C_b	Pelvic-joint-lumped damping of the trunk
k_s	Shoulder linear stiffness		

Dong [9] reported that the application of anti-vibration gloves can lead to a substantial reduction in hand–arm vibration levels, and developed a mechanical equivalent model to assess the vibration isolation performance of such gloves. Xueyan S. Xu [10] proposed an evaluation approach

for quantifying the effectiveness of anti-vibration gloves and demonstrated that these gloves are particularly effective in attenuating high-frequency vibrations. Furthermore, Yao [11] conducted a comprehensive assessment of vibration-damping gloves by considering palm and finger vibration isolation, hand dexterity, and grip retention. Using a weighted performance index to rank the gloves under various operating conditions, the study identified the gel2 and air2 gloves as exhibiting superior overall performance.

Although considerable work has been done to develop hand-arm biodynamic models and to highlight the importance of vibration-damping gloves, simply modeling the fingers as a single mass block is insufficient to fully characterize the distributed vibration response across different parts of the fingers. In this study, a glove–hand–tool coupled model including both the index and middle fingers is established to predict the distributed vibration response of the hand-arm system.

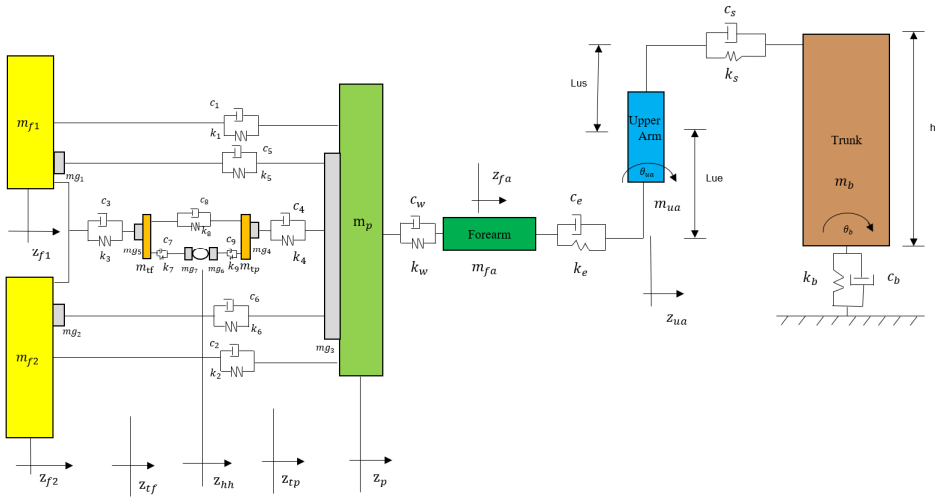

Fig 1. Glove–hand–arm model in the bent-arm posture with an elbow angle of 90°

2. Formulation of Biomechanical Model for The Glove-Hand-Arm System

To better understand and mitigate these risks, transmission rate analyses are conducted to quantify the vibration magnitude transmitted to different regions of the body, including the fingers, wrists, and forearms, when operating vibrating equipment such as hand-held power tools [12] . These analyses are critical not only for evaluating potential health hazards but also for facilitating the selection of appropriate vibration-absorbing gloves tailored to specific work scenarios. In this study, a coupled glove-arm biomechanical model is established to analyze the vibration response under various working conditions, providing a robust framework for evaluating and selecting optimal damping gloves.

2.1. Modeling of Glove-hand-arm System

The glove-hand-arm model, including its inertial, viscous, and elastic properties, is based on the parameters reported by Dong. The glove masses are designated as mg_4 , mg_5 , mg_6 and mg_7, mg_6 and mg_7 correspond to the glove mass attached to the tool handle for finger and palm measurements, while mg_4 and mg_5 represent the glove mass associated with the index finger, middle finger, and palm, respectively. The linear stiffness parameters $k_7$and k_9, together with the corresponding damping coefficients $c_7$and c_9, are used to represent the viscoelastic behavior of the glove material on the finger side and palm side, respectively. Specifically, $k_7$and $c_7$characterize the glove properties associated with the index and middle fingers, while k_9 and c_9 describe those related to the palm region. The glove masses m_{g4}(index and middle fingers) and m_{g5}(palm) are mechanically coupled through the stiffness $k_9$and damping c_9. In addition, other glove segments are incorporated into the model by coupling the auxiliary masses m_{g1} and m_{g3} via the linear stiffness $k_5$and damping c_5, as well as coupling $m_{g2}$and m_{g3}through the parameters k_6 and c_6 . Figure 1 illustrates the biomechanical model of the bent hand–arm system equipped with additional vibration-damping gloves. The linear stiffness parameters k_7 and k_9 , together with the corresponding damping coefficients c_7 and c_9, are used to represent the viscoelastic behavior of the glove material on the finger side and palm side, respectively. Specifically, k_7 and $c_7$characterize the glove properties associated with the index and middle fingers, while $k_9$and $c_9$describe those related to the palm region. The glove masses m_{g4}(index and middle fingers) and m_{g5}(palm) are mechanically coupled through the stiffness $k_9$and damping c_9. In addition, other glove segments are incorporated into the model by coupling the auxiliary masses $m_{g1}$and m_{g3}via the linear stiffness $k_5$and damping c_5, as well as coupling $m_{g2}$and m_{g3}through the parameters $k_6$and c_6. Figure 1 illustrates the biomechanical model of the bent hand–arm system equipped with additional vibration-damping gloves.

The nomenclature for the components shown in Fig. 1 is defined below. The corresponding substructures associated with Fig. 1 are described in the following section.

For the sake of modeling simplicity and to limit the number of rotational degrees of freedom, the effects of rotational stiffness and damping at the wrist joint are not included in the present biodynamic model. The wrist is therefore treated as a kinematic connection without rotational resistance, an assumption that allows the primary vibration transmission characteristics of the hand–arm system to be analyzed without introducing additional model complexity. z_{hh} –Z-axis displacement of the tool handle.

z_{f1}–Translational displacement of the index fingers along the z-axis.

z_{f2}–Translational displacement of the middle fingers along the z-axis.

z_p–Translational displacement of the palm along the z-axis.

z_{fa}–Translational displacement of the forearm along the z-axis.

z_{ua}–Translational displacement of the upper arm along the z-axis.

θ_{ua}–Rotational motion of the upper arm mass with respect to its mass center.

θ_b –Angular displacement of the trunk mass occurring about the pelvic joint.

In the proposed biodynamic representation, the fingers, palm, and forearm are assumed to undergo purely translational motion along the direction of excitation, whereas the upper arm is described using a general planar motion to account for its rotational and translational characteristics. This modeling assumption reflects the different kinematic behaviors of the individual segments of the hand–arm system. As illustrated in Fig. 1, the overall system is formulated as a nine-degree-of-freedom model along the z-axis, enabling a detailed description of vibration transmission through the hand–arm structure. The corresponding equations of motion governing the dynamic behavior of the model are presented in Equation (5).

2.2. Transmissibility Analysis of the Model

To analyze the propagation of vibrations within the hand–arm system, the proposed model is utilized to predict the dynamic responses induced by a displacement excitation applied at the tool handle along the z-axis. This formulation allows the vibration transmission behavior of different segments of the hand–arm system to be evaluated in a systematic manner. The corresponding equations of motion governing the system dynamics are formulated as follows:

$$[M]\{\ddot{z}\} + [C]\{\dot{z}\} + [C]\{z\} = \{F\} \quad (1)$$

In the above formulation, $[M]$, $[C]$, and $[K]$denote the $(n \times n)$mass, damping, and stiffness matrices, respectively. The vector $\{F\}$ represents the $(n \times 1)$ generalized force vector, while $\{z\}$ corresponds to the $(n \times 1)$ generalized displacement vector. Here, $n$denotes the number of degrees of freedom of the system, which is equal to 9 for the bent-arm configuration. A harmonic displacement excitation is applied at the tool handle, and the imposed displacement is expressed as $z_{hh} = z_{hh}e^{j\omega t}$. Based on these assumptions, the equations of motion governing the biodynamic model can be written as:

$$\{z(jw)\} = \left[[k] - w^2[m] + jw[c]\right]^{-1}\{f\} \quad (2)$$

For the bent-arm configuration, the vibration transmissibility response is obtained as

$$T_{f1}(jw) = \frac{z_{f1}(jw)}{z_{hh}(jw)},\ T_{f2}(jw) = \frac{z_{f2}(jw)}{z_{hh}(jw)} \quad (3)$$

$$T_{wz}(jw) = \frac{z_w(jw)}{z_{hh}(jw)},\ T_{ez}(jw) = \frac{z_e(jw)}{z_{hh}(jw)}, T_{sz}(jw) = \frac{z_s(jw)}{z_{hh}(jw)} \quad (4)$$

Here, T_{f1}, T_{f2}, T_w, T_e, and T_s denote the vibration transmissibility responses of the index finger, middle finger, wrist, elbow, and shoulder, respectively. The variables z_{f1}, z_{f2}, z_w, z_e, and z_s correspond to the respective displacements of the index finger, middle finger, wrist, elbow, and shoulder along the z-axis.

2.3. Identification of Model Parameters

The data used in this study consist of vibration transmission rates measured at the wrist, elbow, and shoulder in the bent-arm position, within a target frequency range of 2.5–500 Hz. The average response under an excitation of 5.25 m/s² serves as the target output for the modeling process. Since experimental results have demonstrated that handgrip force and push force have a significant impact on vibration transmission, measurements were carried out using a grip force of 30 N and a push force of 50 N, in accordance with the recommendations of ISO 10819.

The vibration-damping glove used in this study is Air1, which offers excellent isolation of high-frequency vibrations and can effectively reduce vibration transmission to the palm, meeting the requirements of the ISO 10819 standard. This makes it suitable for reducing hand vibration exposure risks in high-frequency vibration environments. The mass parameters of the Air1 glove are shown in the table 2.

The equations of motion were solved using MATLAB to obtain the vibration transmission. Model parameters were identified and optimized by minimizing the composite squared error. between the biodynamic measurements and the model response, utilizing a particle swarm optimization algorithm. The following transmission rate fits are shown for index finger, middle finger, wrist, elbow, and shoulder.

The parameters of the glove-arm-model are shown in Figure 2.

Table 2. Inertial data for the glove

Mass(Kg)	Air1
mg_1	0.0107
mg_2	0.0107
mg_3	0
mg_4	0
mg_5	0.0673
mg_6	0
mg_7	0

3. Results and Discussion

In this study, the glove–hand–arm system is subdivided into multiple structural units, and the coupling of the index and middle fingers is explicitly incorporated into the model, enabling a more refined simulation of vibration transmission characteristics. Compared with previous models in the literature that simplify the fingers as a single mass block, the proposed model can more accurately predict the distributed vibration responses at different locations, such as the index finger, middle finger, palm, wrist, elbow, and shoulder. Experimental results demonstrate that the model shows a high degree of agreement with actual measurement data in the frequency range of 2.5–500 Hz, particularly below 100 Hz, where the predicted and measured trends are almost identical. These findings fully validate the effectiveness and practical value of the model in evaluating the vibration attenuation performance of anti-vibration gloves.

Comparison with literature data Adewusi 2009 [5] , Dong confirms the validity of the developed model. However, minor discrepancies are observed in the shoulder region, likely due to simplifications in the model or individual variability in anatomical properties. Overall, the simulation results verify the capability of the biomechanical model to accurately predict the vibration isolation performance of damping gloves under realistic working conditions.

Table 3. The model parameters were identified by minimizing the target responses using a particle swarm optimization algorithm

Stiffness parameters	value	Damping Parameters	value
k_1(N/m)	48907.1	c_1(Ns/m)	5
k_2(N/m)	134643	c_2(Ns/m)	111.6
k_3(N/m)	18624.1	c_3(Ns/m)	5
k_4(N/m)	100	c_4(Ns/m)	299.9
k_5(N/m)	29459	c_5(Ns/m)	215
k_6(N/m)	300	c_6(Ns/m)	5.1
k_7(N/m)	64388.5	c_7(Ns/m)	124.3
k_8(N/m)	57475.8	c_8(Ns/m)	5
k_9(N/m)	305.3	c_9(Ns/m)	269.7
k_w(N/m)	66000	c_w(Ns/m)	210
k_e(N/m)	53081.7	c_e(Ns/m)	142.6
k_s(N/m)	300	c_s(Ns/m)	305
K_e(Nm/rad)	60000	C_e(Nms/rad)	5.1
K_s(Nm/rad)	41966.5	C_s(Nms/rad)	5
K_b(Nm/rad)	300	C_b(Nms/rad)	5

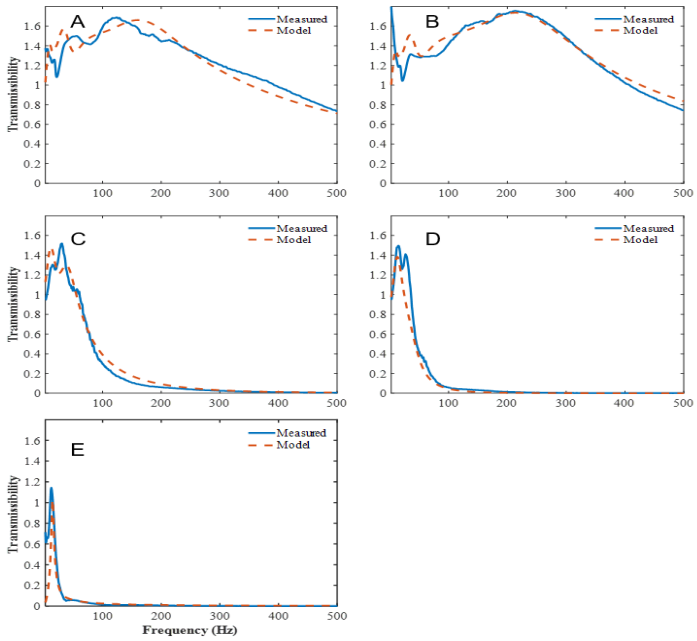

Fig 2. Fitting results of the transmissibility for different parts: A Index finger, B Middle finger, C Wrist, D Elbow, E Shoulder

References

[1] Chowdhry R, Sethi V. Hand arm vibration syndrome in dentistry: A review[J]. Current Medicine Research and Practice, 2017, 7(6): 235-239.J. Clerk Maxwell, A Treatise on Electricity and Magnetism, 3rd ed., vol. 2. Oxford: Clarendon, 1892, pp.68–73.

[2] Handford M, Lepine K, Boccia K, et al. Hand-arm vibration syndrome: Workers' experience with functional impairment and disability[J]. Journal of Hand Therapy, 2017, 30(4): 491-499. Rakheja S, Wu J Z, Dong R G, et al. A comparison of biodynamic models of the human hand–arm system for applications to hand-held power tools[J]. Journal of Sound and Vibration, 2002, 249(1): 55-82.

[3] Rakheja S, Wu J Z, Dong R G, et al. A comparison of biodynamic models of the human hand–arm system for applications to hand-held power tools[J]. Journal of Sound and Vibration, 2002, 249(1): 55-82.

[4] Dong J H, Dong R G, Rakheja S, et al. A method for analyzing absorbed power distribution in the hand and arm substructures when operating vibrating tools[J]. Journal of sound and vibration, 2008, 311(3-5): 1286-1304.

[5] Adewusi S A, Rakheja S, Marcotte P, et al. Vibration transmissibility characteristics of the human hand–arm system under different postures, hand forces and excitation levels[J]. Journal of sound and vibration, 2010, 329(14): 2953-2971.

[6] Adewusi S, Rakheja S, Marcotte P. Biomechanical models of the human hand-arm to simulate distributed biodynamic responses for different postures[J]. International Journal of Industrial Ergonomics, 2012, 42(2): 249-260.

[7] Dong R G, Welcome D E, Xu X, et al. A model for simulating vibration responses of grinding machine-workpiece-hand-arm systems[J]. Journal of Sound and Vibration, 2018, 431: 276-294.

[8] Wang Z, Qiu Y, Zheng X, et al. Biomechanical models of the hand-arm system to predict the hand grip forces and transmitted vibration[J]. International journal of industrial ergonomics, 2022, 88: 103258.

[9] Dong R G. A method for assessing the effectiveness of anti-vibration gloves using biodynamic responses of the hand-arm system[J]. The Shock and Vibration Digest, 2006, 38(4): 343-344.

[10] Xu X S, Welcome D E, Warren C M, et al. Development of a finger adapter method for testing and evaluating vibration-reducing gloves and materials. Measurement (Lond.). 2019; 137: 362–74[EB/OL].

[11] Yao Y, Rakheja S, Marcotte P. A methodology for integrated performance analyses of vibration reducing gloves[J]. International Journal of Industrial Ergonomics, 2021, 85: 103174.

[12] Sun Y, Bochmann F, Eckert W, et al. Quantitative Assessment of Work-related Hand-arm Vibration Exposure Among Workers in the Construction, Underground Coal Mining, Wood Working, and Metal Working Industry: The German Hand-arm Vibration Study[J]. Safety and Health at Work, 2025, 16(1): 97-104.